LIQUID TRANSPORT IN COMPOSITE CELLULOSE–SUPERABSORBENT FIBER NETWORKS

David R. Schuchardt[1] and *John C. Berg*

Department of Chemical Engineering BF-10
University of Washington
Seattle, WA 98195

(Received March 1990)

ABSTRACT

Wicking flow of water is examined in composite networks of cellulose and carboxymethyl cellulose (CMC) fibers. The rate of advance of water through paper strips and fluff pads of varying composition is reported, while dynamic electrotensiometry is used to measure the wetting and swelling characteristics of the individual cellulose and CMC fibers. Cellulose fibers swell to a small degree almost instantaneously, while CMC fibers swell to more than twice their original diameter over a period of several minutes.

The Lucas-Washburn capillary model adequately describes the imbibition of a nonswelling reference liquid (*n*-octane) in all of the fiber networks examined. The imbibition of water, however, deviates significantly from Lucas-Washburn kinetics when CMC is present, because of the long-term swelling of the CMC fibers. The net pore restriction effected by fiber swelling is quantified by a "permeability factor," defined as the ratio of the wicking-equivalent radius in the swollen state to that in the unswollen state. A modified capillary model is developed, based on individual fiber swelling characteristics, which describes observed deviations from the Lucas-Washburn model.

Keywords: Wicking, absorbency, superabsorbents, fiber swelling, Lucas-Washburn theory, gel blocking.

INTRODUCTION

Wood pulp, cotton, and other cellulosic fibers have long been used in the construction of absorbent products. Liquid uptake in these structures is driven by capillary action, and because the fibers themselves usually swell to only a small extent, liquid retention occurs primarily in the interfiber pores. While wood pulp is the most economical material for these applications, much effort has been made in recent years to enhance product performance through the addition of "superabsorbents." These may consist of naturally occurring polymers (such as chitosan or guar gum) or various synthetic polymers (Chen et al. 1985). Typically, composite absorbent structures are produced from mixtures or layers of cellulosic fibers and a superabsorbent. The superabsorbent may be incorporated into the structure as separate fibers, flakes, needles, or powders, or they may be grafted or coated onto the cellulosic fibers (Chatterjee and Nguyen 1985).

Superabsorbents are used to increase the liquid capacity and retentivity of the absorbent structure. They are typically capable of absorbing up to 20 times their weight in water without being solvated, holding much of the water in the polymer network. This swelling results in either an overall expansion of the structure or in the partial filling of the pore spaces between the fibers. Liquid transport is governed both by capillary action in the interfiber pore spaces and by diffusion

[1] Currently with the Boeing Airplane Company, P.O. Box 3707, Seattle, WA 98124.

Wood and Fiber Science, 23(3), 1991, pp. 342–357

of the liquid through the superabsorbent. The two mechanisms are coupled in that the diffusion of the liquid into the superabsorbent generally reduces the dimensions of the interfiber pore space, decreasing the rate of absorption. In the extreme case, a form of "gel blocking" occurs in which the swelling of the superabsorbent completely closes the wicking channels, preventing further wicking and limiting liquid transport to a diffusion process. Thus, compromises must often be made in product design between the rate of absorption and the capacity and retentivity of the structure.

While much qualitative work has been performed in practice to produce successful absorbent products, there is still a need for fundamental understanding of the relationship between fiber swelling and liquid transport rates in fiber networks. The present work seeks to describe the effects of fiber swelling on wicking performance in random fiber networks (either paper strips or air-laid fluff pads) that contain a fibrous form of superabsorbent mixed uniformly in various proportions with cellulose or other wood pulp fibers. It is then sought to correlate the observed absorbency performance of the composite networks with the wetting and swelling characteristics of the individual cellulose and superabsorbent fibers, as measured independently by dynamic electrotensiometry (a Wilhelmy technique).

MATERIALS AND METHODS

Two types of wood pulp fibers were used in both single-fiber and wicking experiments: Whatman #4 fibers (referred to as "cellulose" fibers), which are hydrophilic, bleached wood pulp, and Ecomax TMP (Thermo-Mechanical Pulp) fibers, a relatively hydrophobic pulp obtained from the Weyerhaeuser Co., Tacoma, WA. Two types of superabsorbent fibers were used: Aquasorb FC and FR, Hercules Chemical Company, Wilmington, DE. The Aquasorb products are a highly swellable cross-linked sodium salt of carboxymethylated wood pulp fibers, with a degree of substitution of 0.7.

Two types of wicking media (fiber networks) were investigated: paper strips cut from handsheets and air-laid fluff pads. The handsheets were prepared from the various fibers and their mixtures, using the methods and equipment described in TAPPI Method T205 OM81 (TAPPI Standards and Suggested Methods). However, to ensure sufficient homogeneity and mechanical strength, the dry weight was increased to 1.30–1.40 g. Three-dimensional air-laid fluff pads, to more closely approximate the structure of many end-use applications, were prepared using approximately 4 g of mixed fibers in a 5.6-cm-wide cylindrical tube bounded on the bottom with a stainless steel screen. The pads were unbonded fiber networks with a substantially higher porosity than bonded networks such as obtained from the handsheets. Composite pads were made by alternately adding small amounts of each type of fiber to the pad former, ensuring adequate mixing of the fiber types.

The liquids used in the study were water (triply distilled in an all-quartz apparatus) and *n*-octane (Reagent grade), which was chosen as the reference liquid for both the wicking studies and the individual fiber swelling measurements.

Wicking measurements on the paper strips cut from the handsheets consisted of contacting the strip with the liquid in an enclosed glass chamber (to prevent evaporation) and monitoring visually the height of the advancing liquid front as

a function of time. The absorbency of the fluff pads was determined using the FAQ (Fluff Absorbent Quality) tester (Martinis et al. 1981). A constant pressure of 2.5 kPa was applied to the air-laid fiber pad with a plunger from above, and the pad was contacted with the liquid from below. The height of the collapsing pad was then measured as a function of time using an electrical transducer, with up to 200 sample points obtained per second. Plots of liquid front location or pad height vs. time were analyzed as described below.

Wettability and swelling characteristics of individual fibers abstracted from the above strips and pads were determined in order to evaluate their effects on the wicking behavior. Such information was obtained using an adaptation of the Wilhelmy technique, in which the downward force on a solid object (in this case, the fiber) partially immersed in the liquid is measured. As described below, such data obtained for the liquid of interest as well as a fully wetting but nonswelling reference liquid yield values for the contact angle of the liquid against the fiber and its perimeter, as well as changes in perimeter with time, if it swells. While measurements of this general type have long been used for measuring surface tension, it wasn't until 1976 that the instrumentation was sufficiently developed to permit the measurement of the wetting properties of single wood pulp fibers (Young 1976). The method has since been further refined to allow precise dynamic wettability measurements of single wood pulp and other fibers (Miller 1985; Berg 1986). The technique involves suspending a single fiber in a fixed position from the arm of an electrobalance. The fiber penetrates the surface of a liquid, and the liquid surface is made to move up and down along the fiber's axis at a constant interline velocity. The resulting downward force on the fiber, is given by the Wilhelmy equation:

$$F = \sigma P \cos \theta + \Delta mg, \tag{1}$$

where σ is the liquid surface tension, P is the wetted perimeter of the fiber at a given position along the fiber, θ is the contact angle, and Δm is the mass of any liquid absorbed into the fiber above the meniscus. [The negligible buoyancy term is omitted from Eq. (1).] Recently, the technique was applied to elucidate the relationship between single-fiber wettability profiles and wicking behavior in wood pulp fiber networks (Hodgson and Berg 1988). The apparatus is shown schematically in Fig. 1. It is composed of a Cahn electrobalance (Model C-2000, Cahn Instruments, Cerritos, CA) an Inchworm translator (Model CE-2000, Burleigh Instruments, Fishers, NY) and an IBM PS/2 Model 30 microcomputer.

When the fiber is not fully wet out by the liquid, significant hysteresis will occur between the advancing contact angle (θ_A) and the receding contact angle (θ_R), so that $\theta_A > \theta_R$. For cellulosic fibers wet by water or most organic solvents, it is a good assumption that $\theta_R = 0°$ (Hodgson and Berg 1988), and the cosine of the advancing contact angle may be found by taking the ratio of the advancing force to the receding force:

$$\cos \theta_A = \frac{F_A}{F_R}. \tag{2}$$

An accurate value of the perimeter of the fiber is obtained by dividing the receding force by the liquid surface tension. A measure of the degree of fiber swelling is

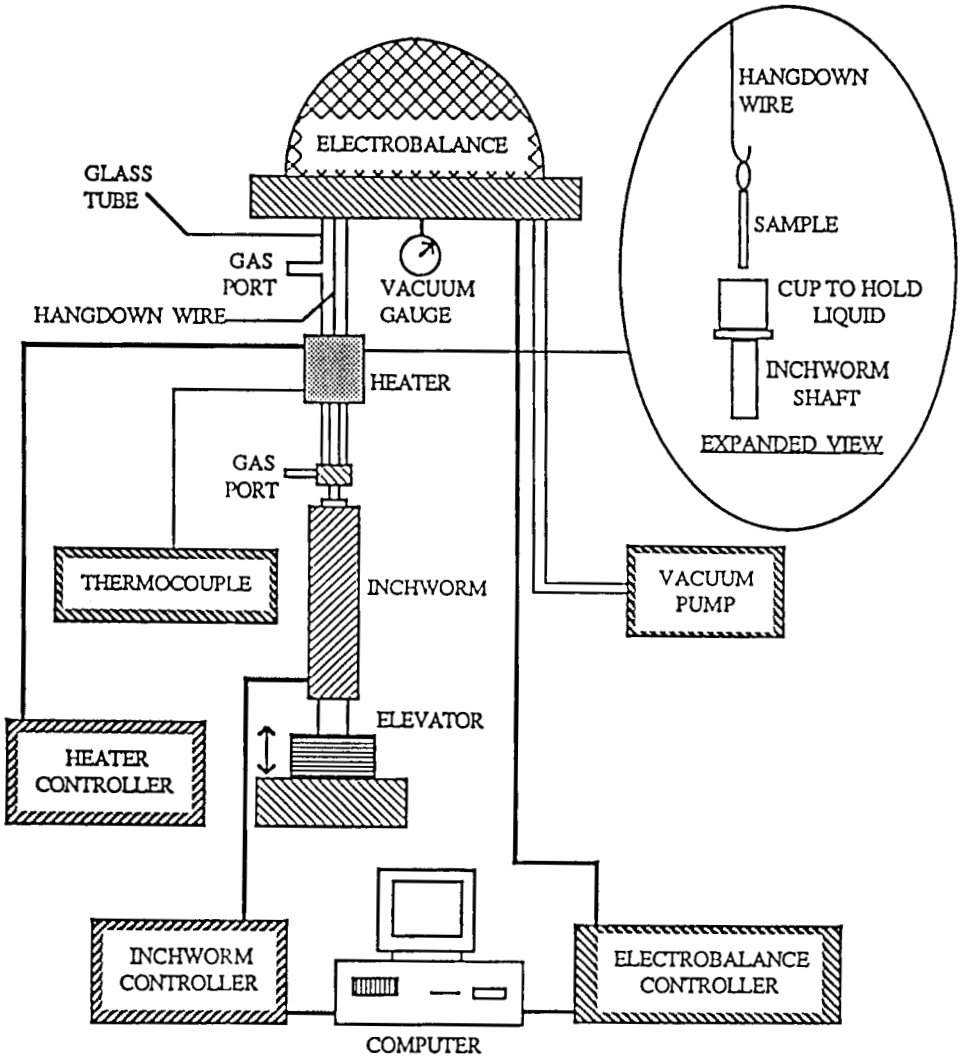

FIG. 1. Schematic diagram of dynamic electrotensiometer.

possible by first measuring the perimeter of the fiber in a nonswelling, fully wetting reference liquid, and then repeating the measurement in the swelling liquid. By measuring the wetting force at a given axial position along a fiber, it is possible to determine the rate at which fiber swelling occurs.

ANALYSIS

The spontaneous uptake of a liquid by a fiber network is usually described by the Lucas-Washburn analysis, which models the complex porous structure of the fiber network as bundles of cylindrical capillary tubes. The model predicts a uniform liquid front that advances linearly with the square root of time:

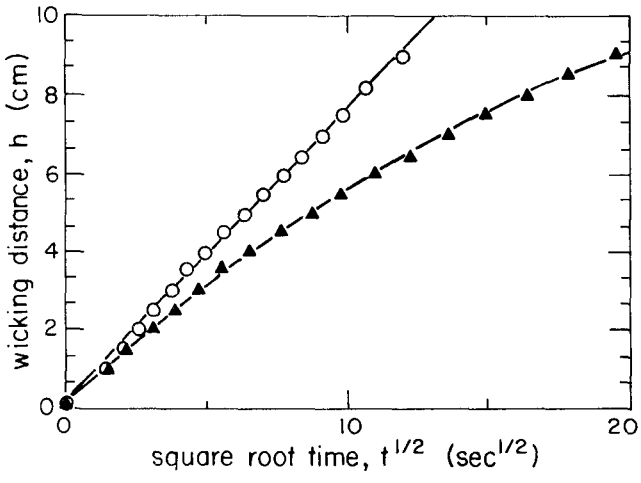

FIG. 2. Lucas-Washburn plot of wicking distance vs. square root of time for *n*-octane (O) and water (▲) in a composite paper strip of 33% CMC/ 67% cellulose.

$$h(t) = \left[\frac{\sigma r_e \cos\theta}{2\mu}\right]^{1/2} t^{1/2} = kt^{1/2}, \tag{3}$$

where σ and μ are the liquid surface tension and viscosity, respectively, r_e is the wicking-equivalent radius, and θ is the liquid contact angle. The collection of factors multiplying $t^{1/2}$, i.e., k, is termed the Lucas-Wasburn constant. In this simple model, the complex geometry of the pore structure is expressed entirely in r_e, which is an empirical geometric parameter. Gravity may be neglected when the pore dimensions are sufficiently small, as in the case of these experiments, except when the equilibrium rise height is approached. In the present case, this equilibrium height is several meters. Other approaches have been taken to account for the actual geometry of pore structures, including the use of interconnected capillary models and diffusion models (Ruoff et al. 1960). However, none of these approaches eliminates the necessity of empirical measurement of some physical parameter describing the rate of liquid uptake. Thus, the simple capillary approach is used in this research, and the changes in r_e are examined to quantify the effects of fiber swelling on the pore structure of the fiber networks. A "Lucas-Washington plot" is prepared by plotting the height of the advancing liquid front as a function of the square root of time. From the slope of this plot, the wicking equivalent radius can be determined if the liquid properties (surface tension and viscosity) are known and if the advancing contact angle of the liquid on the fibers is known. Any changes in r_e reflect the effects of interfiber debonding, as well as swelling and morphological changes (e.g., curling) of the fibers themselves.

A gauge of the net pore restriction caused by fiber swelling is obtained by measuring the Lucas-Washburn constant k for a given fiber network with the swelling liquid (water) and with a nonswelling reference liquid (*n*-octane), and taking the ratio of r_e in the swollen state to that in the (unswollen) reference state. We have termed this ratio the "permeability factor," P_f:

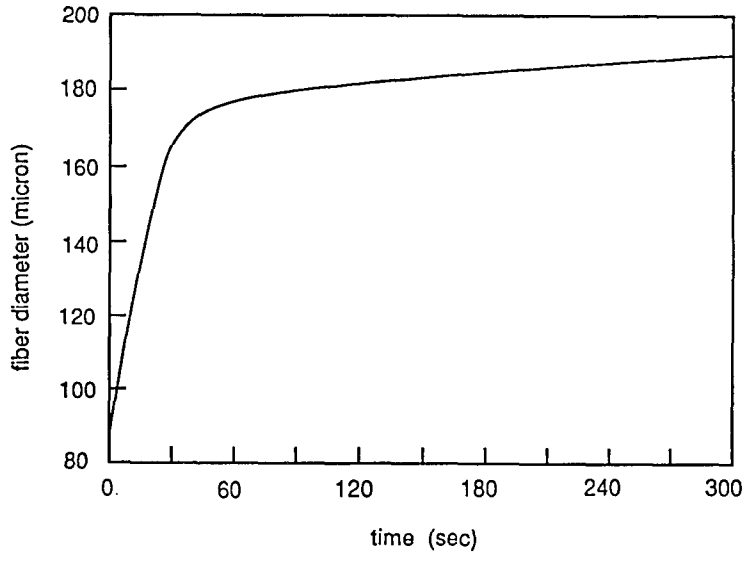

FIG. 3. Time dependence of swelling of a typical CMC fiber by water as measured by electrotensiometer.

$$P_f = \frac{r_{e,swollen}}{r_{e,ref}} = \left[\frac{k}{k_{ref}}\right]^2 \left[\frac{\sigma_{ref}}{\sigma}\right] \left[\frac{\mu}{\mu_{ref}}\right] \left[\frac{\cos \theta_{ref}}{\cos \theta}\right]. \quad (4)$$

Since the reference liquid fully wets the fiber, $\cos \theta_{ref} = 1$. A permeability factor of unity indicates no pore restriction, while a permeability factor of zero corresponds to complete closure of wicking channels.

In cases where superabsorbent swelling does not occur instantaneously, deviations from Lucas-Washburn kinetics are evident. This is a result of a dynamic reduction in the interfiber capillary dimension which occurs as the superabsorbent slowly swells. Figure 2 shows an example of such behavior in the case of water wicking into a cellulose-CMC handsheet strip. By defining a *local* Washburn constant as the local slope of the Washburn plot, it is possible to estimate the wicking-equivalent radius at various points throughout a wicking experiment. The local value of P_f is then computed at various heights, and plots of P_f vs. height are generated for varying handsheet compositions.

This approach is a simplified one in that if the wicking equivalent radius is in fact changing with time, the Lucas-Washburn equation does not integrate to the same form as Eq. (3), and the slope of a h vs. $t^{1/2}$ plot will no longer be directly proportional to the square root of the wicking-equivalent radius. Nevertheless,

TABLE 1. *Swelling measurements of single fibers in water. Reference liquid:* n-*Octane.*

Fiber	Number of samples	% Perimeter increase	Standard deviation	%Volumetric swell
Cellulose	5	10.4	5.0	22
Aquasorb FC	6	114	29	360
Aquasorb FR	5	136	48	460

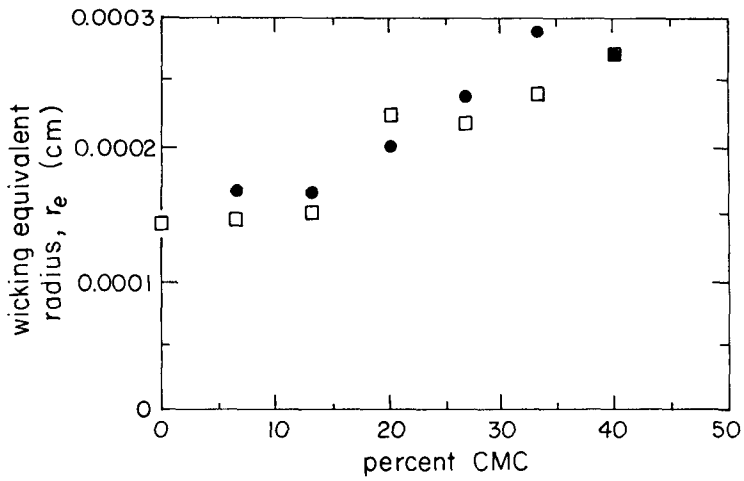

FIG. 4. Wicking-equivalent radius as a function of composition for composite paper strips of CMC and cellulose fibers as measured by the wicking of *n*-octane. (□) Aquasorb FC CMC; (●) Aquasorb FR CMC.

the slope of such a plot indicates the comparative behavior of dynamic changes in the wicking-equivalent radius, and the permeability factor should permit assessment of the extent of pore restriction caused by fiber swelling and comparison of performance among absorbent structures of varying composition.

RESULTS AND DISCUSSION

Single-fiber measurements

Electrotensiometry experiments showed that the cellulose and CMC fibers all had advancing contact angles very near to 0° in water. The TMP fibers, however, were quite hydrophobic; the four fibers tested had a mean advancing contact angle in water of 62° ± 3°.

The results of the single-fiber swelling measurements are shown in Table 1. The percent perimeter increase is the increase in the average fiber perimeter measured in water compared to that measured in octane. The standard deviation of the mean, σ_m, is included as a measure of the uncertainty in these values. The volumetric swell is calculated assuming that no swelling occurs in the axial direction of the fiber, as has been verified by cellulosic fibers (Stamm 1964). The TMP fibers showed negligible swelling by water. Large variations were observed in the degree of swelling of the CMC fibers. Such variability may be attributed to varying degrees of carboxymethylation and crosslinking which are present from fiber to fiber.

Because of the chemical heterogeneity of the CMC fibers, a wide spectrum of swelling rates was also observed. A representative force trace indicating the rate of fiber swelling in water is shown in Fig. 3. Most of the CMC fibers exhibited a very high rate of swelling for the initial 15–60 seconds of immersion, followed by a slow, roughly linear increase in perimeter for periods ranging from three minutes to over twenty minutes. The primary importance of these swelling mea-

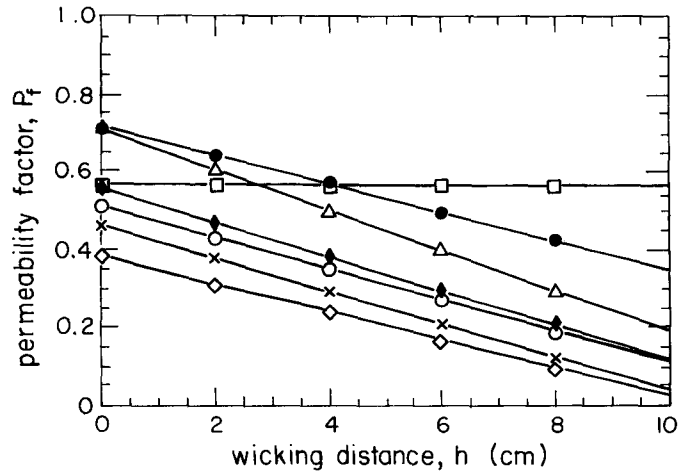

FIG. 5. Permeability factor vs. wicking distance for water in composite paper strips of cellulose and Aquasorb FC CMC fibers. (□) 0% FC; (●) 6.7% FC; (△) 13% FC; (◆) 20% FC; (○) 27% FC; (×) 33% FC; (◇) 40% FC.

surements in the present context is the fact that the process occured over a period of time comparable to that of the wicking experiments.

Wicking in two-dimensional fiber networks (paper strips)

All of the cellulose-CMC and TMP-CMC handsheet strips exhibited classical Lucas-Washburn behavior for the imbibition of *n*-octane. Figure 4 is a plot of the wicking-equivalent radius measured in octane as a function of handsheet composition for these systems. The observed increases in r_e with increasing CMC content indicated an opening of the structure by the CMC fibers. Since the handsheets were wet formed, the superabsorbent fibers were in their swollen state. When the sheets were subsequently dried, these fibers shrank, leaving open spaces in the network which were evident in electron micrographs (Schuchardt 1989).

The wicking-equivalent radii for the two types of CMC were nearly identical. This similarity was expected, since the two types are of the same external dimensions and produced in the same manner. They differ primarily in the degree of cross-linking between the carboxymethyl cellulose chains.

The wicking of water into the 100% cellulose and 100% TMP strips obeyed Lucas-Washburn kinetics, with straight-line correlation coefficients ranging from 0.999 to 1.000. For the cellulose strips, the measured value of P_f was 0.564, indicating a reduction in the wicking-equivalent radius of about 44%. The TMP strips had an average P_f-value of 0.820, which corresponds to only an 18% reduction in r_e. This suggests that even a small degree of fiber swelling (10% perimeter increase for Whatman #4 cellulose fibers) may effect a sizable reduction in the wicking-equivalent radius. The small reduction in the TMP strips was attributed to a slight consolidation of the fiber structure.

The measured permeability factors are plotted as a function of wicking distance for varying fiber compositions in Figs. 5–7. Graphis of this type provide a comprehensive view of the effect of handsheet composition on the pore restriction

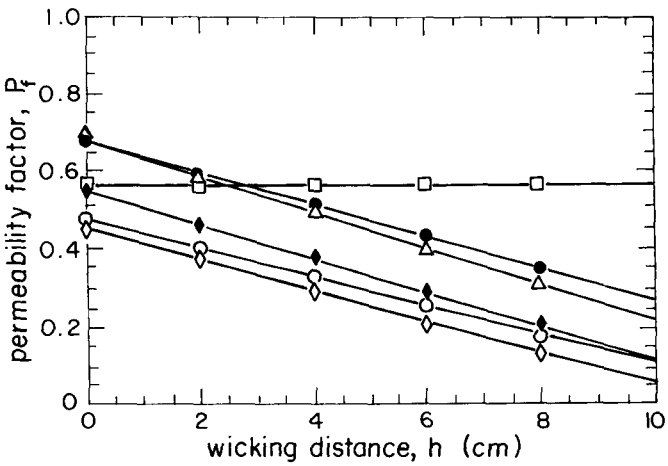

FIG. 6. Permeability factor vs. wicking distance for water in composite paper strips of cellulose and Aquasorb FR CMC fibers. (□) 0% FR; (●) 6.7% FR; (△) 13% FR; (◆) 20% FR; (○) 27% FR; (◇) 33% FR.

caused by fiber swelling. Determination of the strip thickness with a micrometer caliper before and after wicking revealed only a slight (<5%) change in thickness, indicating that the fiber swelling occurred primarily at the expense of the interfiber spaces. Considering first the cellulose-CMC systems in Figs. 5 and 6, several interesting conclusions may be drawn. The slope of each line is equal to the change in permeability factor with respect to wicking distance, which is proportional to the change in wicking-equivalent radius with respect to h. The slope of the line for 100% cellulose handsheets is of course zero, indicating instantaneous swelling of the fibers and an invariant r_e.

1. Each of the handsheets containing CMC had a constant negative slope, which indicates a regular decrease in r_e with height. Since the magnitude of this slope is a measure of the rate at which r_e is decreasing, it was surprising that for all CMC compositions, the slope was approximately the same. One might have expected an increase in slope with CMC content.

2. The P_f for 100% cellulose handsheets (0.564) was a baseline to which the effect of CMC content could be compared. When P_f was above this value (e.g., a 13% Aquasorb FC handsheet at penetration distances less than 2.5 cm) the wicking-equivalent radius was actually greater than that of a 100% cellulose handsheet, and wicking was enhanced. Conversely, when P_f fell below 0.564, pore restriction caused by fiber swelling produced a decrease in wicking performance.

3. There was no appreciable difference in the performance of the two types of CMC. This was foreshadowed by individual fiber swelling measurements which indicated similar degrees of swelling for both fiber types.

The situation with the TMP-CMC composites was complicated by the fact that an independent measurement of the effective contact angle, θ', of water against the *mixture* of fibers is not possible. The wicking results for these composites are thus shown in Fig. 7 as plots of a modified permeability factor, viz. $P_f \cos \theta'$, as a function of composition and penetration distance. They showed the same trends

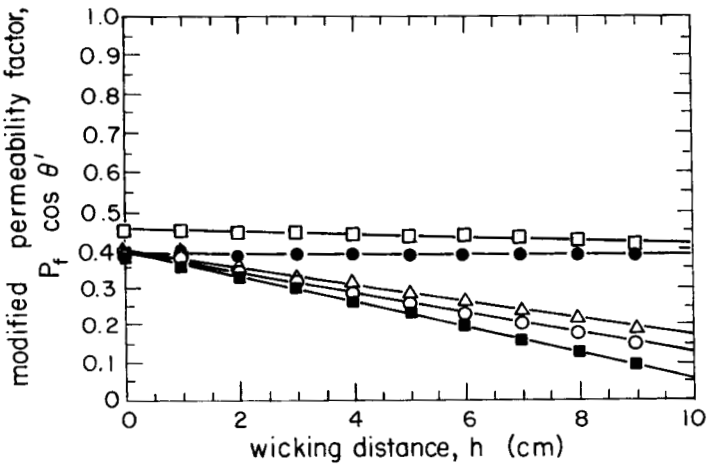

FIG. 7. Modified permeability factor, $P_f \cos \theta'$, vs. wicking distance for water in composite paper strips of TMP and Aquasorb FC CMC fibers. (□) 0% FC; (●) 10% FC; (△) 20% FC; (○) 30% FC; (■) 40% FC.

as the cellulose-CMC composites, but the enhancement in wicking rates at lower CMC content was absent.

Equilibrium water retention was measured in the wicking experiments, since this value reflects the primary advantage offered by the superabsorbent. Figure 8 is a plot of water retention as a function of handsheet composition and shows that water retention, measured as the weight of the saturated strip divided by its dry weight, was roughly a linear function of CMC content. Within the limits of experimental error (caused by variation from handsheet to handsheet), Aquasorb FC and FR had nearly the same water retention characteristics. TMP-CMC strips

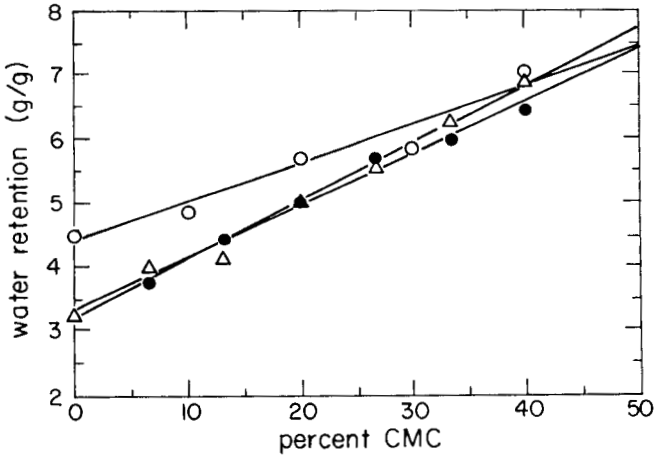

FIG. 8. Water retention in composite paper strips. (●) FC CMC/Cellulose; (△) FR CMC/Cellulose; (○) FC CMC/TMP.

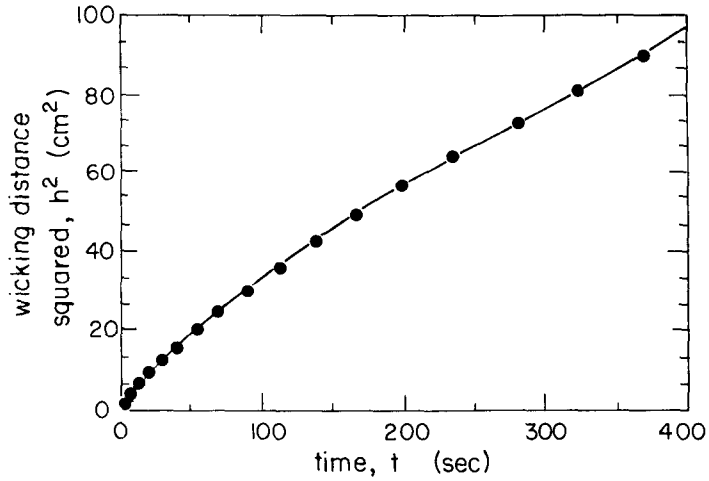

FIG. 9. Wicking distance squared vs. time for water in a composite paper strip of 13% FC CMC/Cellulose. Points are data; smooth curve computed from Eq. (7).

had a slightly higher water retention at lower CMC content, but the two systems were about equal at higher CMC content.

Plots of the type of Figs. 5–8 should be of use in the design of absorbent structures where the performance requirements, such as penetration distance, rate of uptake, liquid retention, and composition must be balanced against each other to achieve an optimum design. It would be necessary, however, to generate the plots for the specific fiber systems and absorbent structures intended for use, since wicking rates in handsheets (for example) may not be indicative of behavior in other structures.

To describe the observed deviations from Lucas-Washburn kinetics during water imbibition into cellulose-CMC fiber networks, a simple modification of the capillary model is proposed, which is consistent with observed swelling rates of single CMC fibers. The model, like that of Lucas and Washburn, is based on viewing the fiber network as an assemblage of cylindrical capillary tubes. In it, however, the effective capillary radius is a function of time and position for the portion of the structure which has been wet by the liquid. The effects of fiber swelling are thus represented as a progressive constriction of the interfiber pore space with time. Since this constriction takes place only after the walls have been wet by the liquid, the advancing meniscus constantly "sees" the initial capillary radius r_o.

Neglecting the net flux of liquid into the capillary walls, and ignoring any axial diffusion through the walls, the Lucas-Washburn equation is re-derived as follows:

$$\frac{dh}{dt} = \frac{r_h^2}{8\mu}\left[\frac{\Delta p}{h}\right] = \frac{r_h^2}{8\mu}\left[\frac{2\sigma \cos\theta}{r_o h}\right], \tag{5}$$

where $\Delta p/h$ is the effective pressure gradient, and r_h is the effective hydrodynamic radius behind the advancing liquid front. The latter is a function of time, and r_o is the capillary radius "seen" by the meniscus. The approach taken is to approx-

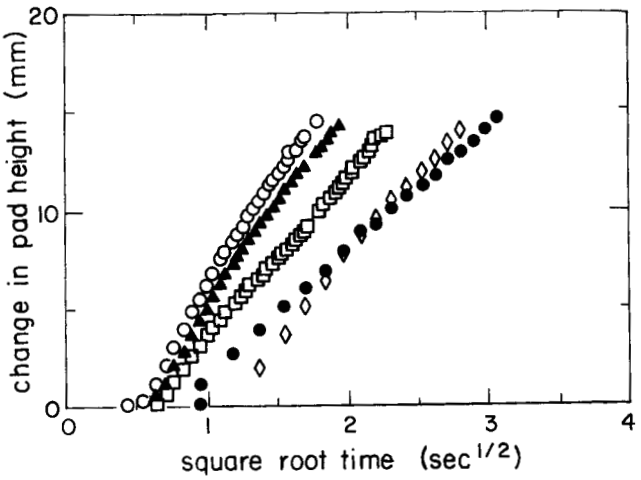

FIG. 10. Wicking results for water in composite fluff pads of Cellulose and TMP fibers. (○) 100% Cellulose; (▲) 75% Cellulose/25% TMP; (□) 50% Cellulose/50% TMP; (◇) 25% Cellulose/75% TMP; (●) 100% TMP.

imate r_h as a linear function of time, and to presume that this is an acceptable approximation over the time period of a wicking experiment;

$$r_h = r_o - at \tag{6}$$

The constant "a" expresses the rate of constriction. With the introduction of this assumption, the integral form of the modified capillary model is:

$$h(t) = \left[\frac{r_0\sigma \cos\theta}{2\mu}\right]^{1/2}\left(t - \frac{a}{r_0}t^2 + \frac{a^2}{3r_o^2}t^3\right)^{1/2} \tag{7}$$

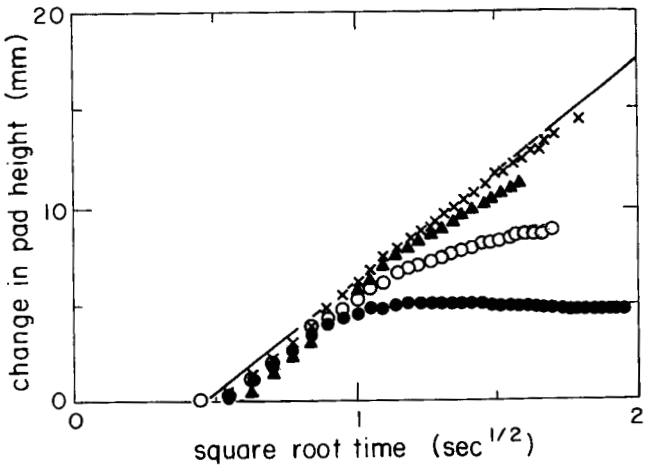

FIG. 11. Wicking results for water in composite fluff pads of Cellulose and CMC fibers. (×) 100% Cellulose; (▲) 75% Cellulose/25% CMC; (○) 50% Cellulose/50% CMC; (●) 25% Cellulose/75% CMC.

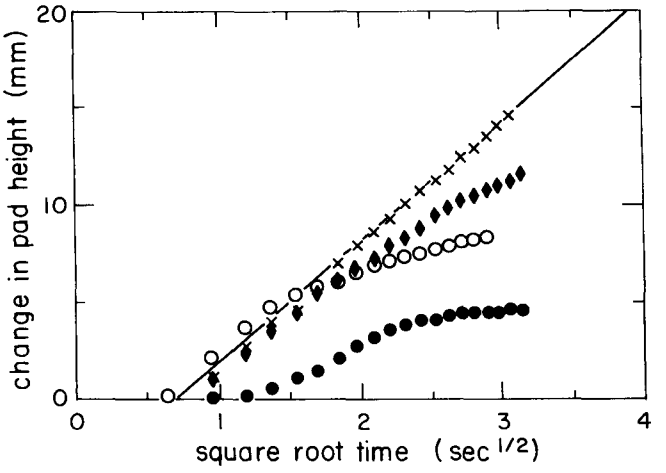

FIG. 12. Wicking results for water in composite fluff pads of TMP and CMC fibers. (×) 100% TMP; (◆) 75% TMP/25% CMC; (○) 50% TMP/50% CMC; (●) 25% TMP/75% CMC.

Plots of h^2 vs. t were prepared from wicking data for each composition of cellulose-Aquasorb FC CMC handsheets and compared to computations based on Eq. (7) using the best-fit values of r_0 and a. A representative plot of this type is shown in Fig. 9. The best-fit parameters were found with a non-linear search routine. Considering all the data, the average values of r_o and a were $0.88 \pm 0.22 \times 10^{-4}$ cm and $0.84 \pm 0.36 \times 10^{-7}$ cm/sec, respectively, but the values obtained for the individual strips did not vary systematically with CMC content. The values of r_o were, as expected, somewhat less than the r_e-values obtained using octane (as shown in Fig. 4) due to the instantaneous swelling of the cellulose fibers. The average a is approximately an order of magnitude less than rate of CMC fiber diameter increase indicated for the slow stage of swelling shown in Fig. 3, a reasonable value.

Wicking in three-dimensional fiber networks (fluff pads)

FAQ data were analyzed by plotting the difference between the initial pad height and the measured pad height ($h_o - h$) against the square root of time, as shown in Figs. 10–12. A large offset is present in the intercepts of these plots, which is in part due to a wetting delay, but primarily the result of a systematic error in defining the time at which absorption begins. The interpretation of these data is

TABLE 2. *Strike-through times for composite fluff pads (sec).*

Composition	System		
	Cellulose/TMP	Cellulose/CMC	TMP/CMC
100/0	1.4	1.4	5.6
75/25	2.2	1.2	5.6
50/50	3.2	1.3	5.3
25/75	3.3	2.0	5.3
0/100	5.6	—	—

dependent on the fiber system. In fluff pads below critical density, which do not contain highly swellable superabsorbent fibers, it is reasonable to assume that the rate of liquid penetration in the loose fiber bed is directly proportional to the rate of pad collapse. This is the case in the cellulose-TMP composite pads. When the advancing contact angle is known, as in the 100% cellulose pads and the 100% TMP pads, a value of the wicking-equivalent radius can be calculated from the FAQ data. For the 100% cellulose pads, $r_e = 3.5 \times 10^{-4}$ cm, and for the 100% TMP pads, $r_e = 4.8 \times 10^{-4}$ cm. The wicking-equivalent radius cannot be calculated for mixtures of cellulose and TMP fibers, since θ is unknown. When superabsorbent fibers are incorporated into the fluff pads, it is difficult to relate directly the rate of liquid uptake to the rate of pad collapse or expansion.

A somewhat more quantitative measure of performance is the strike-through time, which is the time required for complete liquid penetration to the top of the pad. Strike-through times for each of the fiber systems tested are shown in Table 2. The absorbency curves for the cellulose-TMP composite fluff pads, Fig. 10, are fit well by straight lines in each case, indicating an adherence to Lucas-Washburn kinetics. The strike-through times for these pads increased regularly as the TMP content was increased. This decrease in the rate of absorption was caused by the combined effects of increasing the average effective contact angle and altering the wicking-equivalent radius by changing the pore structure of the pad. However, since the wicking-equivalent radii for 100% cellulose and 100% TMP pads did not differ by a large amount, it would appear that any changes occurring in r_e had a lesser impact on the absorption rate than the changes in the effective contact angle.

The results of the FAQ measurements of cellulose-CMC composite pads are shown in Fig. 11. It is significant that relatively minor variations from Lucas-Washburn kinetics were exhibited in the fluff pad containing 25% CMC, while handsheets of higher CMC content displayed very pronounced deviations. Two factors may have influenced this behavior. First, the porosity of the fluff pads was many times greater than that of handsheets, so a relatively smaller reduction in the capillary dimension is associated with the same degree of fiber swelling. Second, the time period for the FAQ absorption was only a few seconds, which does not allow for complete swelling of the CMC fibers.

It is important to note that a downturn in a plot of $(h_o - h)$ vs. $t^{1/2}$ may have been caused by either a decrease in the rate of advance of the liquid front or a physical expansion of the wetted portion of the pad. The latter case was indicated dramatically in the 25% cellulose/75% CMC pad, which reached a point in the absorption curve where the slope was zero, and any pad collapse near the advancing liquid front was offset by an expansion behind the front. As the absorption proceeded, the slope of the curve became negative, and a net swelling of the fluff pad occurred. From Table 2, the time required for liquid strike-through is seen to decrease with low CMC additions, and then steadily increase with CMC content.

The shapes of the absorption curves for the TMP-CMC composite pads (shown in Fig. 12) are qualitatively similar to those for the cellulose-CMC system, although the time required for strike-through was much greater and was not dependent on composition. Apparently, any increase in hydrophilicity caused by the CMC fibers is offset by a decrease in pore size of the dry pad as well as constriction of the capillaries by fiber swelling.

CONCLUSIONS

The complex absorbency characteristics of composite systems consisting of wood pulp and superabsorbent fibers reflect the simultaneous effects of individual fiber wetting and swellability. Experiments on the wicking performance of both paper strips and fluff pads of varying proportions of these materials together with independent experiments on the wettability and swellability of the individual fibers have revealed the dependence of absorbency on the composition of such structures together with a rationalization for the observed behavior.

The Lucas-Washburn model is found to provide a good description of wicking flow when individual fiber swelling is not extensive and occurs rapidly. The incorporation of superabsorbent (CMC) fibers into fiber networks causes significant deviations from Lucas-Washburn kinetics when water is used as the imbibing liquid. The deviations observed are attributable to the long-term swelling of the CMC fibers, which results in a dynamic reduction in the effective interfiber pore dimensions of the structure. In these composite systems, the rate of advance of the liquid front is accurately described by a modified capillary model, in which the hydrodynamic radius of the capillary decreases linearly with time.

The use of the permeability factor, P_f, defined as the ratio of the effective pore radius when the fibers are swollen to that which is measured using a nonswelling reference liquid, provides a convenient means for assessing the changes in the wicking performance brought about by fiber swelling. The permeability factor is a function of penetration distance when there are dynamic changes in the wicking-equivalent radius, and plots may be generated relating P_f to penetration distance for varying fiber compositions. The information presented in plots of this type should be useful in balancing performance requirements in the design of absorbent products.

ACKNOWLEDGMENT

The authors gratefully acknowledge the financial support of the Johnson & Johnson Company and to Mr. Surya Wiryana, who performed many of the experiments.

REFERENCES

BERG, J. C. 1986. The use and limitations of wetting measurements in the prediction of adhesive performance. Pages 23–46 *in* L. Salmén et al., eds. Composite systems from natural and synthetic polymers. Elsevier, Amsterdam.

CHATTERJEE, P. K., AND H. V. NGUYEN. 1985. Mechanism of liquid flow and structure property relationships. Pages 29–84 *in* P. K. Chatterjee, ed. Absorbency. Elsevier, Amsterdam.

CHEN, C. C., J. C. VASSALO, AND P. K. CHATTERJEE. 1985. Synthetic and natural polymers. Pages 197–251 *in* P. K. Chatterjee, ed. Absorbency. Elsevier, Amsterdam.

HODGSON, K. T., AND J. C. BERG. 1988. Dynamic wettability properties of single wood pulp fibers and their relationship to absorbency. Wood Fiber Sci. 20(1):3–17.

MARTINIS, S., J. L. FERRIS, P. J. BALOUSEK, AND M. P. BEETHAM. 1981. Absorption of liquids by dry fiber networks. TAPPI Annual Mtg. Preprint No. 7-3, Chicago. Pp. 1–8.

MILLER, B. 1985. Experimental aspects of fiber wetting and liquid movement between fibers. Pages 121–147 *in* P. K. Chatterjee, ed. Absorbency. Elsevier, Amsterdam.

RUOFF, A. L., G. H. STEWART, H. K. SHIN, AND J. C. GIDDINGS. 1960. Diffusion of liquids in insaturated paper. Kolloid Z. 173:14–20.

SCHUCHARDT, D. R. 1989. The effects of fiber swelling on liquid transport in fibrous media. M.S. thesis, University of Washington, Seattle, WA.

STAMM, A. J. 1964. Wood and cellulose science. Pp. 215–216. Ronald Press Co., New York.
TAPPI STANDARDS AND SUGGESTED METHODS. Atlanta, GA. v. (loose leaf).
YOUNG, R. A. 1976. Wettability of wood pulp fibers. Wood Fiber 8(2):120–128.